Nonionic Star Polymers with Upper Critical Solution Temperature in Aqueous Solutions

Journal:	*Polymer Chemistry*
Manuscript ID	PY-ART-02-2022-000216.R1
Article Type:	Paper
Date Submitted by the Author:	30-Mar-2022
Complete List of Authors:	Aliakseyeu, Aliaksei; Texas A&M University College Station, Materials Science and Engineering Hlushko, Raman; Texas A&M University, Materials Science and Engineering Sukhishvili, Svetlana; Texas A&M University, Department of Materials Science and Engineering

Nonionic Star Polymers with Upper Critical Solution Temperature in Aqueous Solutions

Aliaksei Aliakseyeu[1], Raman Hlushko[1] and Svetlana A. Sukhishvili[1]*

[1]*Department of Materials Science & Engineering, Texas A&M University,*

College Station, Texas 77843, USA

Abstract

We report synthesis of temperature-responsive linear and star poly(2-ureido aminoethyl methacrylates) (PUEMs) of matched molecular weights, their phase transitions in aqueous solutions and interactions with hydrogen bonding and hydrophobic small molecules. PUEMs with number of arms up to 8 were synthesized via the activator regenerated by electron transfer atom transfer radical polymerization (ARGET ATRP) technique using the core-first approach. The degrees of branching were determined using gel permeation chromatography (GPC) equipped with the multi-angle laser light scattering and viscometry detectors. The polymer molecular architecture had a neglectable effect on the upper critical solution temperature (UCST) behavior in aqueous solutions, while the presence of a strong hydrogen-bonded acceptor – dimethyl sulfoxide (DMSO) – suppressed the transition temperature for both linear and star UCST polymers. Importantly, star PUEMs showed an enhanced ability of trapping model drug molecules – proflavine and pyrene. In particular, an increase in polymer branching led to 4.5-fold more efficient proflavine trapping and stronger binding of pyrene molecules within the hydrophobic domains of star polymers below their UCST. The trapped molecules could be then fully released from the star polymers upon temperature increase, demonstrating a potential for controlled delivery applications.

Introduction

Upper critical solution temperature (UCST) behavior is not readily achieved with aqueous polymer solutions because these transitions are controlled enthalpically and involve interpolymer interactions which are often suppressed in water.[1-4] However, UCST are observed for some polymers which are able to solubilize at higher temperatures in aqueous solutions as a result of breaking interpolymer electrostatic (in the case of polyzwitterions) or hydrogen bonding interactions.[2, 4] Previous studies showed that UCST transition temperature of linear polymers can be tuned by varying polymer concentration,[5-6] molecular weight,[7-9] composition (for copolymers),[6, 9-12] solution pH[8, 10, 12] or salt concentration.[6, 12-14] The use of UCST responsive blocks in linear copolymers enables temperature-triggerable block copolymer micelles (UCST

BCMs) useful for on-demand drug delivery systems[15] and temperature responsive smart layer-by-layer (LbL) coatings.[16-19] While LbL coatings provide a perfect environment for the micelles supporting their reversible temperature-triggered drug release,[17-18] individual UCST BCMs disintegrate above the transition temperature when not in the coating, limiting their use for drug delivery in solutions.

Polymers with non-linear topologies can be used as an alternative to UCST block copolymers micelles. Linked through covalent bonds, non-linear polymers (e.g. star polymers) do not disintegrate in solution and show promising drug delivery features due to high compactness and enhanced local concentration of polymer units.[20-21] For example, in nonpolar solvents, non-temperature-responsive amphiphilic 6- and 12-arm star poly(oligo (ethylene glycol)methacrylate-*b*-lauryl methacrylate)s showed increased encapsulation of polar molecules such as rhodamine and bovine serum albumin as compared to their linear counterparts.[22] Similarly, dendritic star polyacrylamide exhibited enhanced drug loading capacity of doxorubicin and sodium diclofenac in aqueous solution.[23] Star block copolymers with pH responsive cores and LCST poly(isopropyl acrylamide) (PNIPAM) corona were also used for delivery of antimicrobial agents to plant leaves and roots.[24] Interestingly, an increase in PNIPAM block length in these star polymers constrained release of a model drug from the poly(acrylic acid) core. In another example, pH rather than temperature was used to control drug release from star polymers. Specifically, cyclodextrin-core poly(2-(diisopropylamino)ethyl methacrylate)-*b*-poly[(ethylene glycol) methyl ether methacrylate] (CPO) star polymers were able to efficiently encapsulate doxorubicin (DOX) and showed its pH-triggered release.[25] Additionally, DOX-loaded CPO showed highly selective cytotoxicity to cancer cells, demonstrating relevance of this system to biomedical applications.

However, studies of UCST behavior of star polymers and its use for controlling dye (or drug) trapping and release are rare. Theoretical and experimental studies of polystyrene stars in different organic solvents found a decrease in the UCST transition temperature with an increase in number of arms for polymers with matched molecular weights.[26-30] This was related to fewer unfavorable polymer-solvent contacts[31] and a stronger contribution of entropy to the Flory-Huggins interaction parameter χ for more branched polymers.[32] Yet the above studies were performed for non-aqueous solutions of non-polar polymers.

In aqueous solutions of polar polymers, a different set of interactions plays a role, such as hydrogen bonding, dipole-dipole interactions between the polymer units, and competition for binding/hydration with water molecules. Previous studies of UCST star polymers explored the effect of branching on their temperature-responsive behavior. In one of such studies, Zhou *et.al.* synthesized linear and 32-arm star polypeptides and converted them to UCST responsive polymers via partial ureido modification.[33] For polymers with matched molecular weights and degrees of ureido modification, it was shown that star polymers had higher UCST than their linear counterparts, and the transition temperature could be additionally tuned by the degree of ureido modification. In another study, Li *et.al.* reported polyzwitterionic linear and star polymers synthesized using the arm-first approach and showed that an increase in number of arms at a fixed arm length led to higher UCST.[34] Interestingly, a differently designed experiment in which the overall molecular weight rather arm length was fixed, resulted in the opposite conclusion of a higher UCST for linear polyzwitterionic polymers.[34] Finally, with random UCST copolymers of poly(acrylamide-*co*-acrylonitrile) whose transition temperatures could be tuned via percentage of acrylonitrile units and the overall polymer concentration, an increase in arm length was found to lower the transition temperature.[35] Thus, studies of the effect of branching on UCST transitions in aqueous solution were controversial, and the use of these transition for trapping of small molecules remained unexplored.

Our research aims to explore the effect of polymer topology on UCST behavior and drug trapping properties of star polymers. We used the activators regenerated by the electron transfer atom transfer radical polymerization (ARGET ATRP) technique for synthesis of linear and star poly(2-ureido aminoethyl methacrylate) (PUEM) UCST polymers using the core-first approach. In prior studies, the UCST behavior of PUEMs was demonstrated for linear homopolymers[36] revealing a strong effect of molecular weight and polymer concentration on the transition temperature. Linear PUEM polymers were also incorporated within diblock copolymers to form UCST micelles for controlled drug delivery applications.[37-39] However, temperature-responsive star PUEM polymers remained unexplored. Using polymers with varied number of arms and matched molecular weight, we have studied the dependence of UCST transitions on the polymer branching and the presence of a small hydrogen bonding competitor – dimethyl sulfoxide (DMSO). Moreover, we explored the efficiency of UCST polymers of different molecular

architectures in capturing and releasing model drug molecules – proflavine and pyrene – in response to a temperature trigger.

Materials and methods

Pentaerythritol (PTOL, synthesis grade), dipentaerythritol (DPTOL, synthesis grade) used for synthesis of tetra-functional, hexa-functional initiators were received from Merck. Tripentaerythritol (TPTOL, technical grade) used for synthesis of an octa-functional initiator was purchased from Sigma-Aldrich. Ethyl α-bromoisobutyrate (EtBiB) (98%), α-bromo isobutyril bromide (BIBB) (98%), isopropanol (ACS grade), imidazole (99%), potassium isocyanate (96%), di-tert-butyl dicarbonate (BOC anhydride, 99%), tetrahydrofurane (THF, ACS grade), dimethylformamide (DMF, ACS grade) copper (II) bromide (99%), tris(2-pyridylmethyl)amine (TPMA), tin (II) hexanoate (92.5-100%), hexanes (mixture of isomers, ACS grade), $CDCl_3$, D_2O and d_6-DMSO were purchased from Sigma-Aldrich. 2-aminoethyl methacrylate (min 95%) was purchased from Polysciences and used as received. Aluminum oxide acidic for chromatography (50-200 μM, 60 Å) and aluminum oxide basic for chromatography (40-300 μM, 60 Å) were obtained from Acros Organics. Chloroform (ACS grade), hydrochloric acid (36.5%, ACS grade), sodium bicarbonate (ACS grade), dichloromethane (ACS grade), dimethyl sulfoxide (ACS) and cetyltrimethyl ammonium bromide (CTAB, high purity) were purchased from VWR. Anisole (99%), trifluoroacetic acid (99%), pyrene and pyridine (99%) purchased from Alfa Aesar, and proflavine hydrochloride purchased from MP Biomedicals were used as received. Dialysis tubing (cutoff 3.5kDa) was purchased from Thermo Scientific. Water used in this study was purified with a Millipore Milli-Q system.

Synthesis of a tetra-functional initiator pentaerythritol tetrakis(2-bromoisobutyrate), 4f-BiB: 25 ml of dry dichloromethane, 10 ml (0.129 mol) of dry pyridine and 1 gram (0.029 mol of OH groups) of pentaerythritol were mixed in a flask containing a magnetic bar. The solution was cooled to 0 °C in an iced bath. After cooling, a solution of 7.3 ml (0.06 mol) of BIBB in 25 ml of dichloromethane was added dropwise through a syringe within 30 minutes under vigorous stirring. The reaction mixture was incubated for 24 hours at room temperature, and chloroform was added while the solution was stirred for additional 30 minutes. The resulting solution was triple washed with each of 10% HCl, 5% solution of $NaHCO_3$ and distilled water until pH of the distilled water after washing remained neutral. The resulting solution was sequentially passed through basic and

acidic SiO_2 columns and dried over sodium sulfate overnight. After that, dichloromethane and chloroform were removed by rotary evaporation and the residual liquid containing 4f-BiB was recrystallized in isopropanol. The product was a white solid (3.5 grams, yield 65%). ^{1}H NMR (CDCl$_3$): δ 1.88 (8×s, 24H), δ 4.27 (4×s, 8H) (**Fig. 1A** and **S1**).

Synthesis of a hexafunctional initiator dipentaerythritol hexakis(2-bromoisobutyrate, 6f-BiB: 6f-BiB was synthesized in the same manner as described for 4f-BIB keeping the 2:1 molar ratio of OH-groups in dipentaerythritol to BIBB. The product was a white solid (2.5 grams, yield 58%). ^{1}H NMR (CDCl$_3$): δ 1.88 (12×s, 36H), δ 3.53 (2×s, 4H), δ 4.27 (6×s, 12H) (**Fig. 1A** and **S2**).

Synthesis of octa-functional initiator tripentaerythritol octakis(2-bromoisobutyrate), 8f-BiB: 8f-BiB was synthesized in the same manner as described for 4f-BIB keeping the 2:1 molar ratio of OH-groups in tripentaerythritol to BIBB. The product was a white solid (3.5 grams, yield 57%). ^{1}H NMR (CDCl$_3$): δ 1.88 (16×s, 48H), δ 3.48 (4×s, 8H), δ 4.27 (8×s, 16H) (**Fig. 1A** and **S3**).

Synthesis of 2-(tert-butoxycarbonylamino)ethyl methacrylate (BOC AMA): Protection of 2-aminoethyl methacrylate with the tert-butoxycarbonyl (BOC) group was performed as described elsewhere.[40] Briefly, 8.4 g of sodium bicarbonate (0.1 mol) and 4.14 g (0.025 mol) of 2-aminoethyl methacrylate hydrochloride were dissolved in 100 ml of a THF/water mixture (1:1 by volume) in a 200 ml Schlenk flask. After complete dissolution of the components, the mixture was freeze-thawed to avoid polymerization of the monomer. Then 6.54 g (0.03 mol) of BOC anhydride was added to the frozen solution and the mixture was freeze-thawed again. The flask was immersed in a water bath at 25 °C and left to stir overnight. The solution was then extracted with diethyl ether (3×100 ml) and dichloromethane (3×100 ml). The organic phase was combined, dried under sodium sulfate overnight, and concentrated under vacuum. The concentrate was diluted with dichloromethane and precipitated in cold hexane to remove the polymerized material. After filtration of the polymerized material, the solution was again evaporated under reduced pressure to yield BOC AMA as white crystals (4.3 g, yield 75%). ^{1}H NMR (CDCl$_3$): δ 1.38 (3×s, 9H), δ 1.88 (s, 9H), δ 3.37 (q, 2H), δ 4.15 (t, 2H), δ 4.70 (bs, 1H), δ 5.51 (s, 1H), δ 6.06 (s, 1H) (**Fig. 1B**).
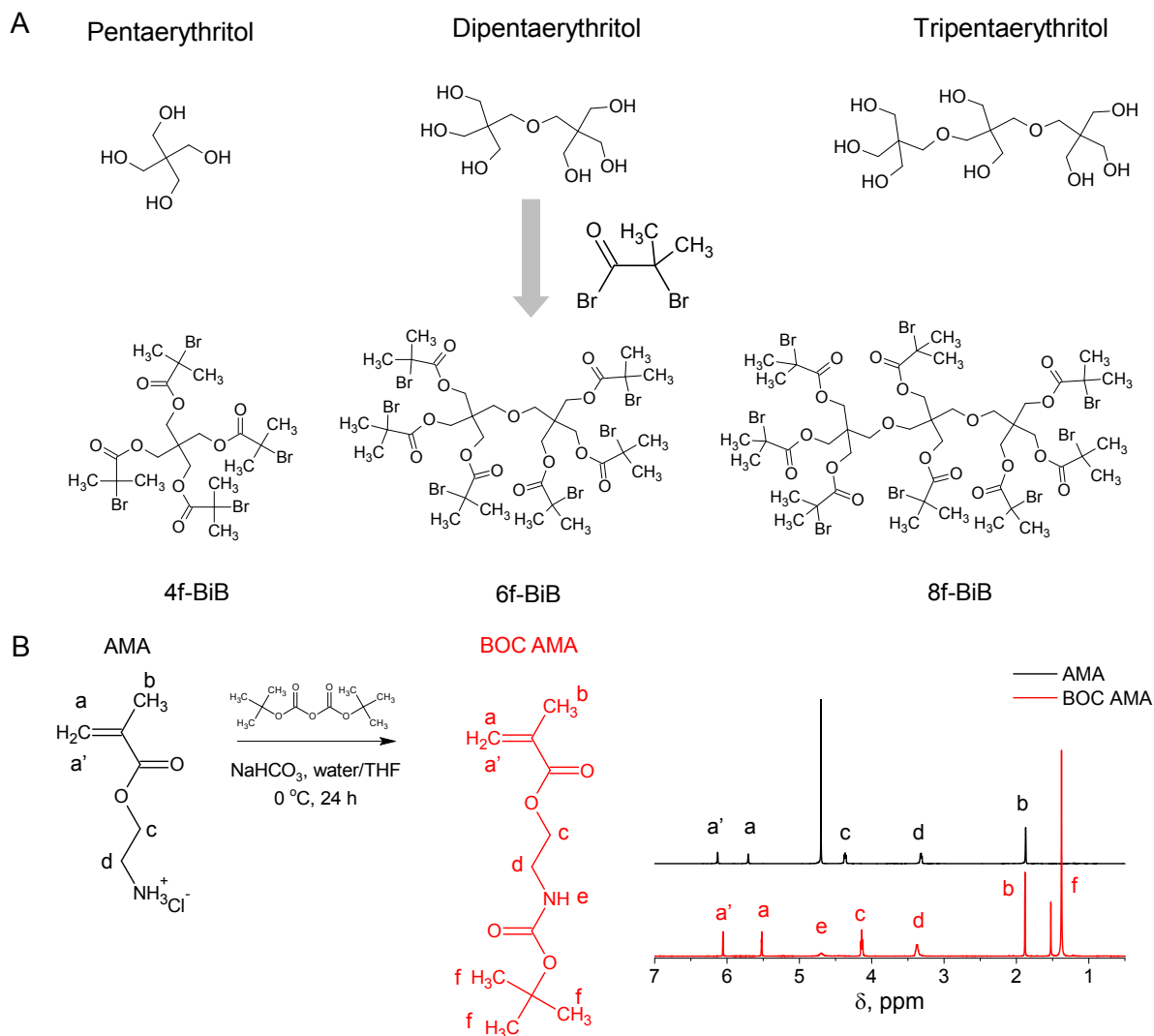
Fig. 1. (A) Chemical structures and the synthetic pathway to 4, 6 and 8-arm ATRP initiators. (B) Synthesis of BOC-protected AMA monomer used for linear and star polymers, and ^{1}H NMR spectra of AMA solution in D$_2$O and BOC AMA solution in CDCl$_3$.

Synthesis of linear and star poly(2-(tert-butoxycarbonylamino)ethyl methacrylate) (BOC PAMA): Linear and star BOC PAMA were synthesized using ARGET ATRP technique which was previously developed for linear methacrylates.[41] In particular, linear functional, tetra-functional, hexa-functional or octa-functional initiator (EtBiB, 4f-BiB, 6f-BiB, or 8f-BiB), copper (II) bromide, TPMA and BOC AMA were dissolved in dry anisole in a Schlenk flask equipped with a magnetic bar. The concentration of the monomer in anisole was constant for all systems (1.7 M). The solutions were freeze-thawed three times. After that, solution of tin (II) hexanoate in

dry anisole was added to the frozen mixtures. The initiator-to-monomer molar ratio shown in Table 1 was maintained at 1:400, while the ratio of Cu(II):TPMA:tin (II) hexanoate was 1:5:10. The ratio of initiator to Cu(II) was adjusted for each system to achieve control of the polymerization rate. The mixture was freeze-thawed two more times to completely remove oxygen, immersed into an oil bath and heated to 40 °C. Polymerization kinetics was monitored by taking aliquots of the solution mixture, followed by gel permeation chromatography (GPC, Tosoh EcoSec) analysis using DMF as an eluent (**Fig. 3** and **Figs. S4-6**). The polymerization was quenched by immersing the flask in liquid nitrogen. The polymer was then precipitated into cold hexane and filtered under reduced pressure. The GPC traces of the final product are shown in **Fig. S7A**.

Table 1. The molar ratio of initiating sites, copper (II) bromide, the ligand, the reducing agent and the monomer to the initiator in the polymerization mixtures.

	Initiator	Initiating sites	CuBr$_2$	TPMA	Sn(OHex)$_2$	Monomer
EtBiB	1	1	0.14	0.7	1.4	400
4f-BiB	1	4	0.2	1	2	400
6f-BiB	1	6	0.3	1.5	3	400
8f-BiB	1	8	0.26	1.3	2.6	400

Determination of dn/dc of linear and star BOC PAMA: Response of a GPC refractive index detector RI (mV) is described by the following equation: $RI = K_{ins} \cdot c_i \cdot V_i \cdot \frac{dn}{dc}$, where K_{ins} is an instrumental constant, mV/ μl, c_i – polymer concentration, g/ml, V_i – injected volume, μl, and $\frac{dn}{dc}$ – refractive index increment, ml/g. The instrumental constant K_{ins} was determined using polystyrene (PS) with M_w = 30 kDA and Đ=1.06 (provided by Wyatt Inc.) and the known value of $\frac{dn}{dc}$ for PS in DMF of 0.159 ml/g. The calibration curve was constructed by injecting 5 - 35 μl volumes of $3.8*10^{-3}$ g/ml solution of PS in DMF (total of 7 injections with 5-μl increments in volume increase). **Fig. S8** shows the plot of RI vs. concentration. Fitting this dependence with the linear equation $RI = a + V_i \cdot b$, where $b = K_{ins} \cdot c_i \cdot \frac{dn}{dc}$ yielded $K_{ins} = 5.74*10^6$ mV/μl.

Solutions of linear and 4-, 6- and 8-arm BOC PAMAs at concentrations 4.5, 4.9, 5.1 and 5.1*10^{-3} g/ml, respectively, were then used to determine dn/dc of these polymers. These solutions were injected at the same volumes as used for the construction of the calibration curve. **Figs. S9&S10 A,B** show plots of RI vs. concentration for linear and 4-, 6- and 8-arm PUEMs, respectively. The linear fits to these dependences shown in **Figs. S9&S10 C,D** and the knowledge of K_{ins} (5.74*10^6 mV/μl) allowed to determine dn/dc for linear and star polymers, which were 0.051, 0.049, 0.05 and 0.048 ml/g for linear, 4-, 6- and 8-arm BOC PAMAs, respectively.

Determination of absolute molecular weight and polymer branching

With the known values of dn/dc for linear and star polymers, absolute molecular weight and polymer branching were determined by performing GPC equipped with a 3-angle laser light scattering (MALLS) detector (Wyatt μDawn TREOS) and a viscometry detector (Wyatt viscostar III). Branching of star polymers was quantified via measurements of intrinsic viscosity enabled by the viscostar III detector. Because of their more compact structure, branched polymers had lower viscosity than linear polymers.[42] This was quantified by the branching ratio g' defined as follows:

$$g' = \left(\frac{[\eta]_{branched}}{[\eta]_{linear}} \right)_M$$

where $[\eta]_{branched}$ and $[\eta]_{linear}$ are intrinsic viscosities for polymers with the same molecular weights. The viscosity-based branching ratio g' is related to the radius-of-gyration-based branching ratio g as $g' = g^e$, where e is a draining parameter ($e = 0.7$ was chosen following recommendations of Wyatt provider). The branching degrees (number of branching points per molecule) determined from these data using Wyatt software were 4.1, 6 and 8 for 4-, 6- and 8-arm BOC PAMA polymers (**Fig. S7B**). We used linear BOC PAMA as a standard to identify the branching points of star polymers. All data processing was performed using ASTRA 7.1.4 software. The number- and weight-average molecular weights, dispersity and number of branching points for linear and star BOC PAMAs are summarized in Table 2 in the Results and Discussion section.

Deprotection of linear and star BOC PAMA: 0.2 gram (0.9 mmol of polymer units) of linear or star BOC PAMA were dissolved in 2 ml of dichloromethane in a 20 ml glass flask containing a magnetic bar. 0.5 ml (6.5 mmol) of trifluoroacetic acid was then added to each solution under

vigorous stirring, and all solutions were stirred for 2 hours. The precipitated polymers were filtered and dissolved in water. Aqueous solutions of the deprotected polymers were placed in the dialysis tubes with a 3.5 kDa molecular weight cutoff and dialyzed against 0.001M HCl solution for 2 days. The dialyzing 0.001M HCl solution was renewed every 12 hours. Upon completion of the dialysis all solutions were freeze-dried to yield white powders of linear and star PAMA. ^{1}H NMR analysis confirmed complete disappearance of the BOC protective groups for the polymers of all molecular architectures (**Fig. 4B** and **Fig. S11**).^{1}H NMR of PAMA (D_2O): δ 0.85-1.1 (bs 3H), δ 1.6-2.0 (bs, 2H), δ 3.25-3.35 (bs, 2H), δ 4.15-4.3 (bs, 2H).

Ureido-modification of linear and star PAMA: 0.1 gram (0.6 mmol of polymer units) of linear or star PAMA were dissolved in a 3% solution of potassium cyanate in 1 M imidazole (pH of the imidazole buffer was 7) in a 20 ml glass flask containing a magnetic bar. All solutions were placed into an oil bath heated to 55 °C and stirred overnight. The solutions were then diluted with 5 ml of water (all solutions remained clear), placed in the dialysis tubes with a 3.5 kDa molecular weight cutoff, and dialyzed against water for 2 days. The dialyzing water was changed every 12 hours. All solutions were freeze-dried to yield white powders of linear or star PUEM. ^{1}H NMR analysis confirmed the formation of ureido-groups for the polymers of all molecular architectures (**Fig. 4B** and **Fig. S11**). ^{1}H NMR of PUEM (d_6-DMSO): δ 0.75-1.0 (bs 3H), δ 1.5-1.9 (bs, 2H), δ 3.24 (bs, 2H), δ 3.88 (bs, 2H). δ 5.68 (bs, 2H), δ 6.2 (bs, 1H).

UV-VIS measurements: Turbidity measurements were performed to explore UCST behavior of linear and star PUEMs in aqueous solutions. Turbidity was measured at a wavelength 620 nm using a Shimadzu UV 2600 spectrophotometer equipped with a temperature-controlled cell connected to a Julabo CORIO CD heating immersion circulator. For studies of UCST behavior 0.1, 0.25, 0.5, 1, 1.5 and 2 mg ml^{-1} solutions of PUEMs in water were adjusted to pH 6. Studies of the effect of dimethyl sulfoxide (DMSO) on the UCST transition temperature were performed with 0.5 mg ml^{-1} solutions of linear and star PUEMs in 0, 0.2, 0.4. 0.6, 0.8 and 1 M DMSO using a cooling rate of 0.5 °C min^{-1}.

Proflavine capture and release studied by fluorescence: For the proflavine capture studies, a 0.8 mg/L solution of proflavine in water was prepared by dissolving 0.2 mg of proflavine hydrochloride in 250 ml of water at pH 6. The mixture was left overnight in a flask wrapped with aluminum foil to fully dissolve proflavine, and then used to prepare 0.5, 1 and 2 mg/ml solution

of linear and star PUEMs in the 5-ml centrifuge tubes. Polymer-free proflavine solutions were used as a control. The solutions were heated at 75 $^{\circ}$C for 2 hours to dissolve the polymers, and placed in the fridge (5°C) overnight to precipitate PUEMs below their UCST transitions. The mixtures with the precipitates were centrifuged for 30 min at 5°C and 15,000 rpm using a Hermle Z216K centrifuge, and 2-ml solutions of supernatants carefully collected, placed in plastic cuvettes and analyzed by measuring fluorescence intensity. Fluorescence emission spectra were recorded for each solution at the fixed excitation wavelength λ_{em}=445 nm. After fluorescence analysis, the supernatant solutions were placed back to the centrifuge tubes and all solutions were heated above their UCST (i.e. to ~65 $^{\circ}$C for 0.5 mg/ml solutions and to ~75 $^{\circ}$C for 1 and 2 mg/ml solutions). Fluorescence measurements were performed using a Shimadzu RF-6000 fluorometer equipped with a temperature-controlled cell connected to a Julabo CORIO CD heating immersion circulator. All experiments were done in triplicate.

For a calibration curve of proflavine fluorescence intensities, 1 mg of proflavine was dissolved in a 10 ml volumetric flask (100 mg/L) to prepare a parent solution that was diluted to obtain 1, 0.5, 0.313, 0.25. 0.156 and 0.1 mg/L solutions for measurements at 5 $^{\circ}$C using the excitation wavelength of 445 nm. **Fig. S12** shows that fluorescence intensity changed linearly with concentration of proflavine.

Pyrene capture and release studied by fluorescence: For pyrene capture studies, a saturated solution of pyrene in water was prepared as follows: 5 mg of pyrene and 20 ml of water at pH 6 were mixed in a flask (pyrene solubility in water at 25 $^{\circ}$C is ~ 0.14 mg/L (0.7 µM)). The mixture was sonicated for 30 min and used to prepare 1 mg ml^{-1} solutions of PUEMs or CTAB. All pyrene-containing polymer solutions were first heated to ~75 $^{\circ}$C (above UCST) to dissolve the polymers, and then cooled to 5 $^{\circ}$C (below UCST) to trigger collapse of PUEMs and trapping of pyrene. All solutions were slightly opalescent but did not form precipitates when stored for 12 h at 5°C degree prior to measurements.

Capture and release of pyrene by PUEMs of different molecular architectures were monitored by measuring the pyrene fluorescence excitation spectra at the emission wavelength λ_{em} of 392 nm. The measurements were performed using a Shimadzu RF-6000 fluorometer equipped with a temperature-controlled cell connected to a Julabo CORIO CD heating immersion circulator. Temperature of the pyrene-PUEM aqueous solutions was changed between 5 $^{\circ}$C and 75 $^{\circ}$C in these measurements.
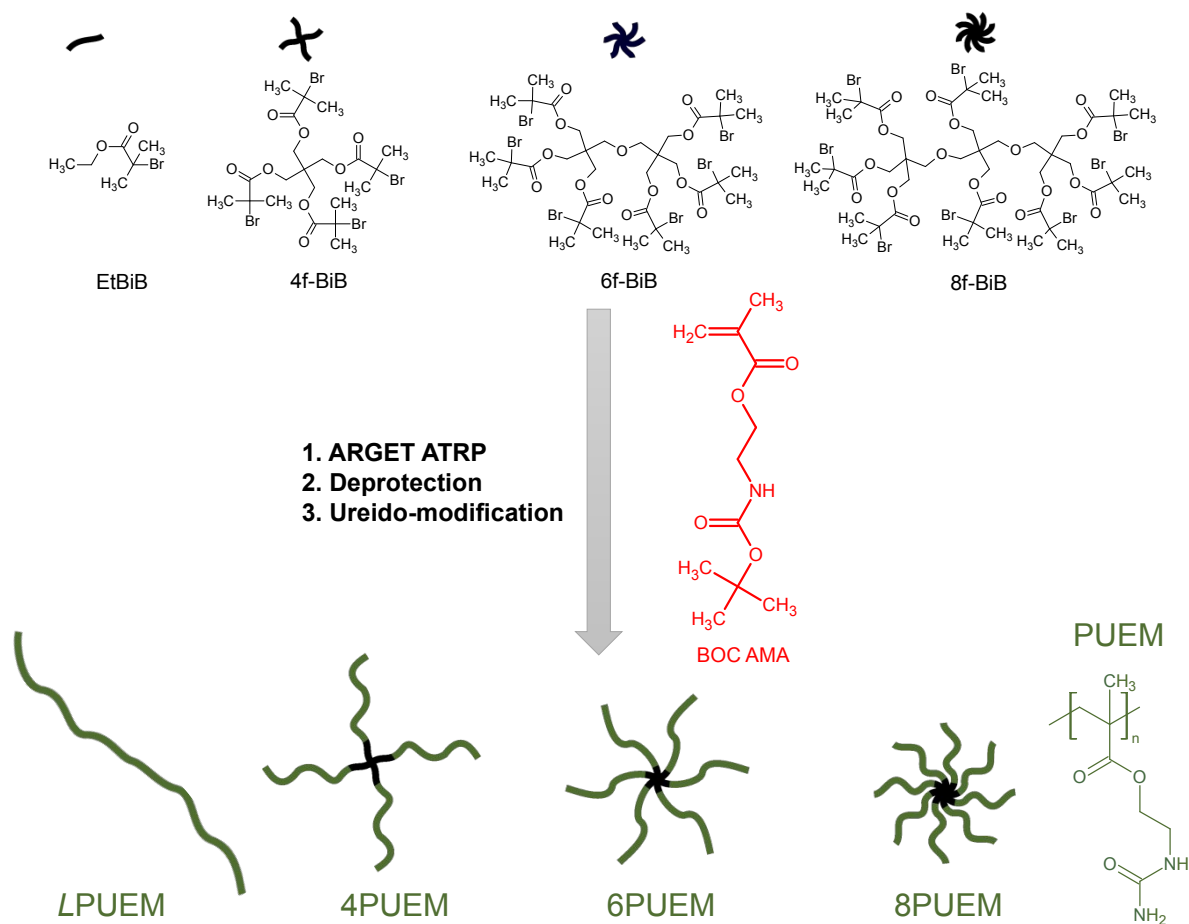
Fig. 2. Schematic representation of synthesis of temperature responsive linear and star PUEMs. *L*PUEM, 4PUEM, 6PUEM and 8PUEM represent linear, 4-arm, 6-arm and 8-arm star PUEMs, respectively.

RESULTS AND DISCUSSION

We first aimed to synthesize a well-defined series of temperature-responsive PUEMs with matched molecular weights and different number of arms. Linear PUEM polymers synthesized via RAFT were earlier reported to exhibit UCST behavior with a negligible effect of salt on its transition temperature (T_{tr}),[36-37] but star PUEMs remained unexplored. Our choice for synthesis of star polymers was the core-first approach, which yields well-defined number of arms, in contrast to a broad distribution of number of arms resulting from the arm-first approach.[20] Furthermore, because star RAFT initiators do not provide good control over polymerization due to the prevailing chain termination reactions,[43] we used ARGET ATRP technique to synthesize star polymers with

low dispersity of arm lengths (**Fig. 2**). In comparison to traditional ATRP, ARGET ATRP is associated with fewer undesirable side reactions[44-45] and requires smaller amounts of organic solvents at the step of polymer purification.[46] The synthesis started from the preparation of a series of mono- and multifunctional ATRP initiators (EtBiB, 4f-BiB, 6f-BiB and 8f-BiB, see **Materials and Methods**) using the procedures similar to those previously used for synthesis of 4f-BiB from pentaerythritol.[47] ^{1}H NMR confirmed successful synthesis of 4-, 6, and 8-arm initiators (**Figs. 1A in Materials and Methods and Figs. S1-S3**). Note that all initiators except for EtBiB were hydrophobic. This prevented us from using water or water-alcohol mixtures previously broadly applied as solvents in RAFT[48-49] or ATRP[50-51] polymerization of 2-aminomethyl methacrylate (AMA) for synthesis of UCST-responsive linear polymers.[36-37] Therefore, in our case, AMA monomer was modified with BOC groups using established procedures.[40] This resulted in improved solubility of the monomer in a variety of organic solvents and allowed for a selective control of solubility of the monomer and hydrophobic multifunctional core ATRP initiators. ^{1}H NMR spectra of AMA and BOC AMA shown in **Fig. 1B in Materials and Methods** confirm successful modification of the monomer.
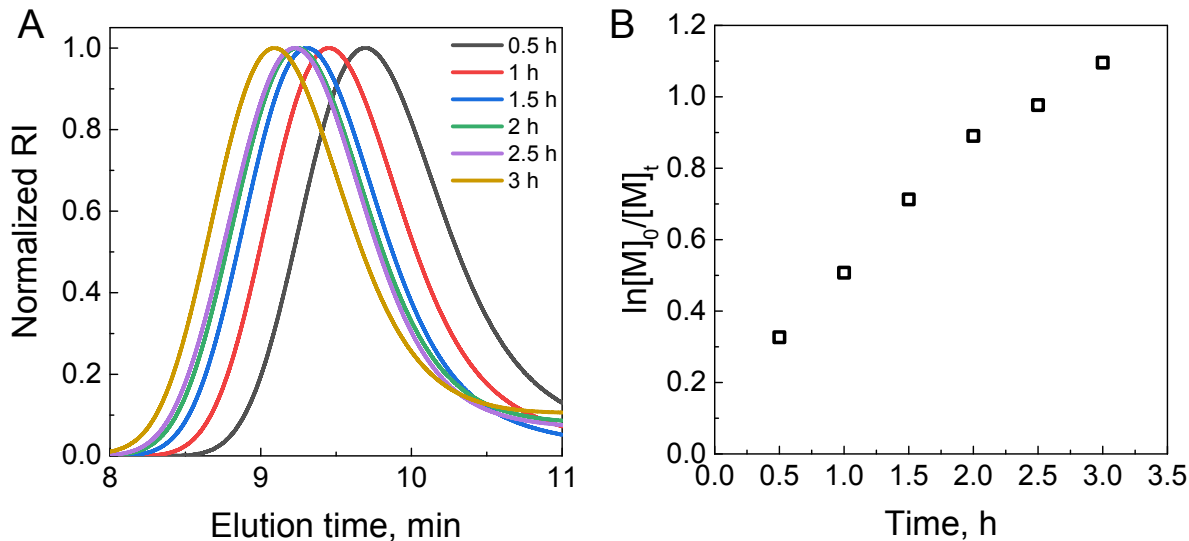

Fig. 3. ARGET ATRP polymerization of 2-BOC AMA using a 4-arm ATRP initiator: (A) GPC traces at different polymerization times; and (B) time evolution of $\ln[M]_0/[M]_t$ during synthesis of 4-arm BOC PAMA.

Fig. 3 shows kinetics of BOC AMA polymerization using 4-arm polymer as an example, while Figs. S4, S5 and S6 illustrate synthesis of linear, 6- and 8-arm polymers, respectively. In all cases, polymerization of BOC-protected AMA was fast, with ~70% conversion reached in less than 3 hours. The linearity of the plot in Fig. 3B shown for synthesis of 4-arm BOC PAMAs confirms the controlled nature of ATRP polymerization. The GPC traces of BOC PAMA polymers after completion of polymerization are summarized in Fig. S7. The use of MALLS and viscometer detectors during GPC analysis enabled determination of the absolute molecular weights and the branching ratios of the BOC-protected PAMAs. Because star polymers were more compact and had lower intrinsic viscosities in comparison to linear polymers of the same molecular weight,[42] the branching ratios could be determined by comparing the absolute molecular masses and intrinsic viscosities of the polymers. Details of the branching analysis are described in the Materials and Methods section and shown in Fig. S7B. Fig. S13 shows that BOC PAMA polymers of the star architecture exhibited lower intrinsic viscosities in comparison to linear BOC PAMA and had branching ratios that matched functionality of the initiators. The molecular characteristics of the synthesized polymers are shown in Table 2.

Table 2. Molecular characteristics of the linear and star BOC PAMAs as determined by GPC in conjunction with light scattering and viscometry analysis.

| Polymer	M_n, kDa	M_w, kDa	Đ	Branching per molecule	Degree of polymerization (DP)	DP per arm
linear	72.1	75.3	<1.1	-	310	-
4 arm	70.3	72.9	<1.1	4.1±0.1	304	76
6 arm	77.7	81.8	<1.1	6.1±0.1	336	56
8 arm	74.5	79.0	<1.1	8.1±0.1	320	40

BOC PAMAs with different molecular architectures were then converted to UCST-responsive polymers (Fig. 4A). Figs. 4 B&C and Fig. S11 show changes in ^{1}H NMR and FTIR spectra of polymers during conversion. The first step of modification involved removal of BOC protecting groups in the acidic conditions to yield PAMAs. ^{1}H NMR spectra confirmed full removal of the tert-butyl group through the disappearance of the BOC methyl group signal (f) in ^{1}H NMR traces (Fig.4B and Fig. S11). Similarly, the removal of the protective BOC group was
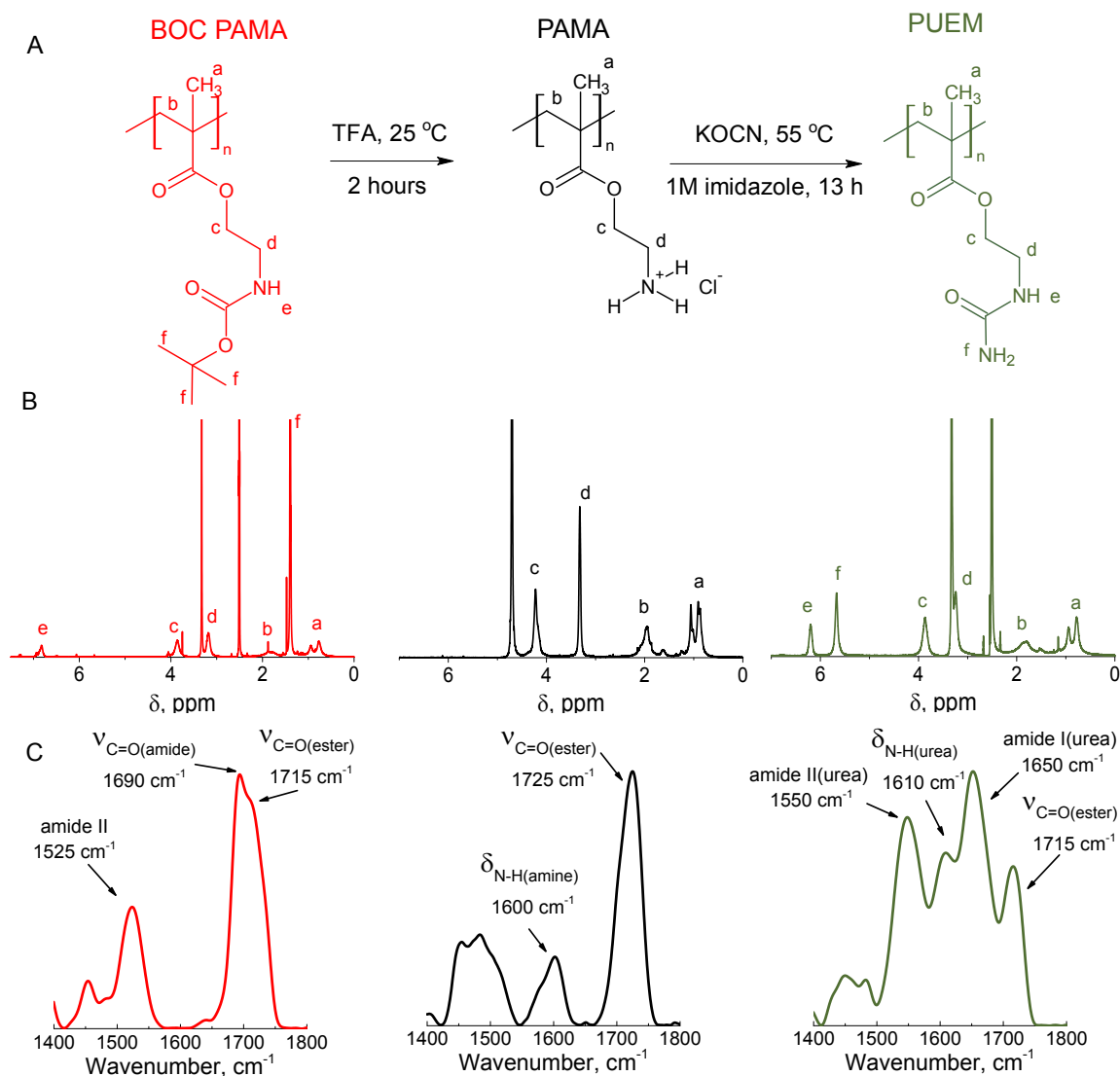
Fig. 4. Conversion of BOC PAMAs to temperature-responsive PUEM polymers: (A) schematic representation of the modification; (B) ^{1}H NMR spectra of 4-arm BOC PAMA (d_6-DMSO), 4-arm PAMA (D$_2$O) and 4PUEM (d_6-DMSO); (C) FTIR spectra of BOC-protected 4-arm BOC PAMA, PAMA and 4PUEM.

also evident in the FTIR spectra of PAMA which indicated the disappearance of the amide I and amide II peaks[52] in the spectra of 4-arm BOC PAMA and the emergence of a new peak at 1605 cm^{-1} which is associated with the deformation vibrations of the primary amino groups[52] (**Fig. 4C**). The deprotected linear and star polymers were then used for ureido-modification to obtain a family of linear and star UCST-responsive polymers (*L*PUEM, 4PUEM, 6PUEM and 8PUEM for linear, 4-arm, 6-arm and 8-arm PUEMs, respectively). The ureido modification was performed in excess

14

of potassium isocyanate to achieve complete conversion and eliminate the effect of incompleteness of the ureido modification on UCST transition temperature.[53] After ureido modification, two new signals at 5.7 ppm (f – bs, 2H) and 6.2 ppm (e – bs, 1H) characteristic of the ureido group of PUEMs emerged in the ^{1}H NMR spectra (**Fig. 4B and Fig. S11**). The equal areas of peaks f and c related to the ureido groups and CH_2 groups in the ethyl spacer, respectively, suggest complete conversion of PAMAs to PUEMs. The FTIR spectra also revealed significant changes in the 1400-1800 cm^{-1} region after ureido modification. In particular, amide I and amide II bands at 1655 and 1550 cm^{-1} characteristic of urea[52] emerged and the band associated with N-H deformation vibrations of the primary amino group[52] shifted from 1600 to 1610 cm^{-1} as a result of ureido modification.
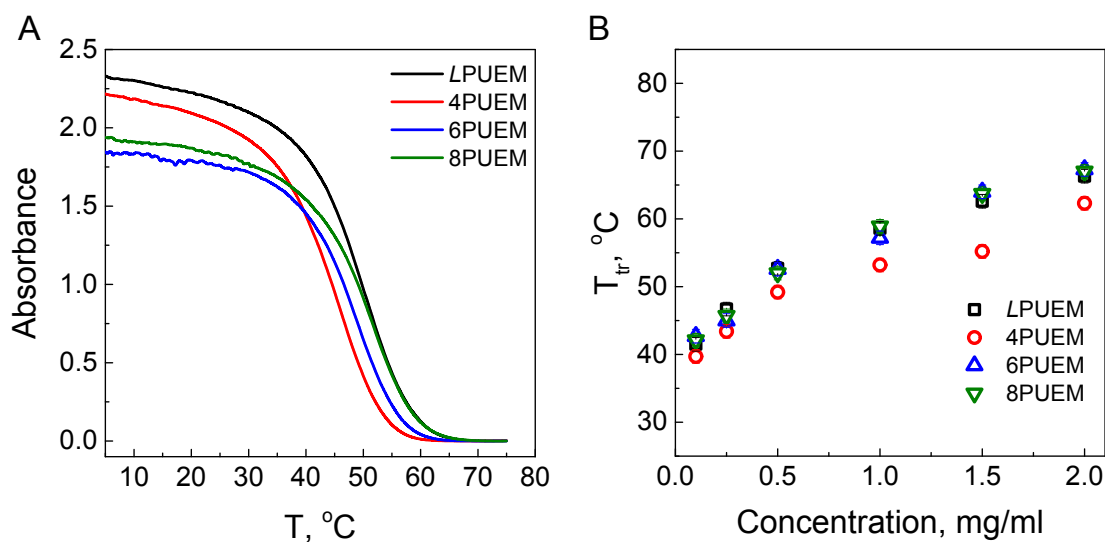

Fig. 5. UCST temperature response of PUEM polymers of different molecular architectures in aqueous solutions at pH 6: (A) Absorbance in 1.0 mg/mL aqueous solutions of 2, 4-, 6- and 8- arm PUEMs measured at 620 nm upon cooling at a rate of 0.5 ˚C/min. (B) UCST transition temperature as a function of polymer concentration for *L*PUEM (squares), 4PUEM (circles), 6PUEM (up-pointing triangles) and 8PUEM (down-pointing triangles). pH of all solutions was adjusted to pH 6.

Fig. 5A shows that the resultant linear and star PUEMs were temperature-responsive in aqueous solutions, as evidenced by changes in turbidity of solutions that were initially heated at 75 ºC and then slowly cooled at a rate of 0.5 ˚C/min. The transition temperature (T_{tr}) was determined from the cross-section of the slope of the increasing absorbance with the temperature scale as shown in **Fig. S14**. Additionally, the width of the transition, which was earlier defined as

the phase transition window (ΔT), can be also considered.[34] Fig. S15A shows that ΔT (determined as shown in Fig. S15B) decreased with polymer concentration, in agreement with an earlier report for hydrogen-bonded linear UCST polymers,[6] and that the trend was similar for the polymers with different molecular architectures. **Fig. 5B** illustrates the effect of polymer concentration and branching on the UCST behavior of linear and star PUEMs. In all cases, the transition temperature gradually increased with polymer concentration. Note that for linear PUEM, the transition temperature (59 °C at a polymer concentration of 1 mg/ml) was higher than that reported in the literature (43 °C at the same concentration).[36] This difference is due to the strong dependence of the transition temperature on the polymer molecular weight. Specifically, while linear PUEMs in the earlier reports were composed of 49 and 100 units and had transition temperatures 21 and 43 °C, respectively,[36] linear PUEM synthesized in this work had a higher molecular weight (DP 310) and therefore showed a higher UCST temperature. In contrast to the strong effect of concentration, the impact of branching was weak, and all polymers except for the 4-arm PUEM showed similar UCST transition temperatures. The lower transition temperature of the 4-arm polymer is probably due to its slightly lower molecular weight (Table 2). A negligible effect of the molecular architecture on UCST transition is possibly a result of compensation of the enthalpic and entropic contributions to the free energy of mixing.
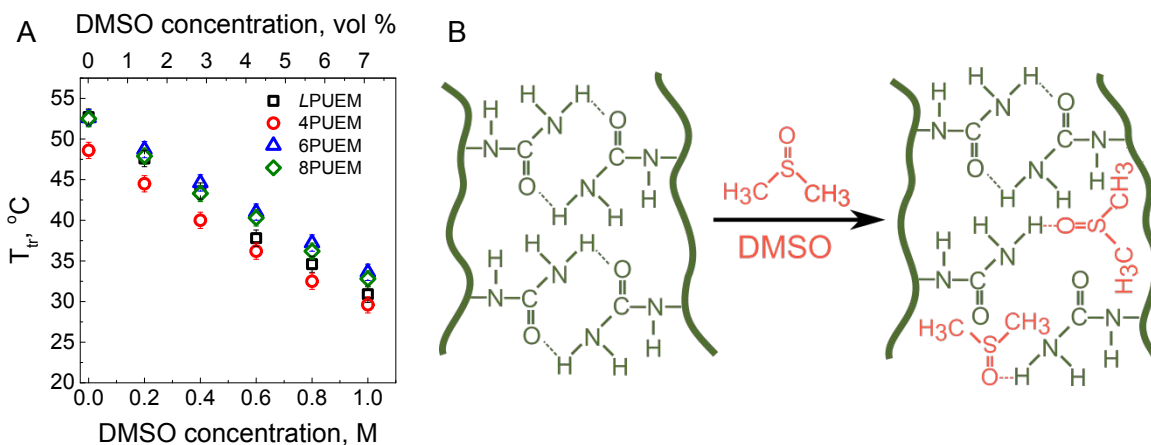
Fig. 6. The effect of DMSO on UCST behavior in 0.5 mg/ml solutions of PUEMs of different molecular architectures: (A) PUEM transition temperatures as a function of DMSO concentration; (B) Schematic representation of disruption of hydrogen bonding between PUEM units by the competing DMSO molecules. Acidity in all solutions was adjusted to pH 6.

16

We further aimed to explore the ability to control UCST behavior of linear and star PUEMs using a strong hydrogen-bonded acceptor – dimethyl sulfoxide, DMSO. Recently, our group showed that DMSO can serve as an efficient hydrogen bonding competitor and impact the binding between hydrogen-bonding polymers in solutions and at surfaces.[54-55] Similarly to the effect of inorganic salts on electrostatic interpolymer complexes, DMSO weakened hydrogen-bonded interpolymer interactions resulting in enhanced polymer diffusion and stronger intermixing within layer-by-layer films.[55] **Fig. 6A** shows that the addition of DMSO to aqueous solutions of linear and star PUEMs led to a gradual decrease of UCST transitions for polymers of all architectures. Note that this trend is opposite to what was observed upon addition of small salts to another type of water-soluble UCST polymers, i.e. polyzwitterions that demonstrate improved solubility due to the anti-polyelectrolyte effect.[2] We believe that lowering the transition temperature occurs as DMSO disrupts inter- and intermolecular hydrogen bonds between ureido units of PUEMs which are involved in UCST response (**Fig. 6B**). A similar competition of DMSO with hydrogen bonding in polymer systems was previously observed by us for poly(vinyl pyrrolidone/poly(methacrylic acid) interpolymer complexes.[55] These data show that the UCST transition temperature in PUEM solutions can be precisely controlled by the addition of DMSO. However, the data in **Figs. 5&6** suggest that PUEM molecular architecture did not impact the temperature transition of these polymers in water and water/DMSO mixtures.

We then hypothesized that despite its negligible effect on the transition temperature, molecular architecture can be important for trapping molecular payloads by the PUEM molecules as they experience a temperature-triggered collapse. Enhanced drug trapping by star polymers was earlier demonstrated for non-temperature responsive polymers.[20, 56-57] UCST polymer systems bring an additional advantage of using temperature as a trigger to control capture and release of small molecules and drugs.[58-60] Many of such systems, however, include block copolymer micelles (BCMs) which require additional crosslinking to suppress their disintegration above UCST in solutions.[58] In contrast, UCST star polymers are unimolecular nanocontainers which do not disintegrate at an increased temperature. To explore the ability of UCST linear and star PUEMs to trap and release drug molecules, we used proflavine hydrochloride (**Fig. 7A**) – a chemical that possesses antibacterial and antiviral properties,[61-62] and emits fluorescence with a maximum at 509 nm (λ_{ex}=445 nm).[63] **Fig. 7A** summarizes the procedure used to assess capacity of trapping. Linear and star PUEMs were first dissolved in proflavine solutions heated above the polymers' transition
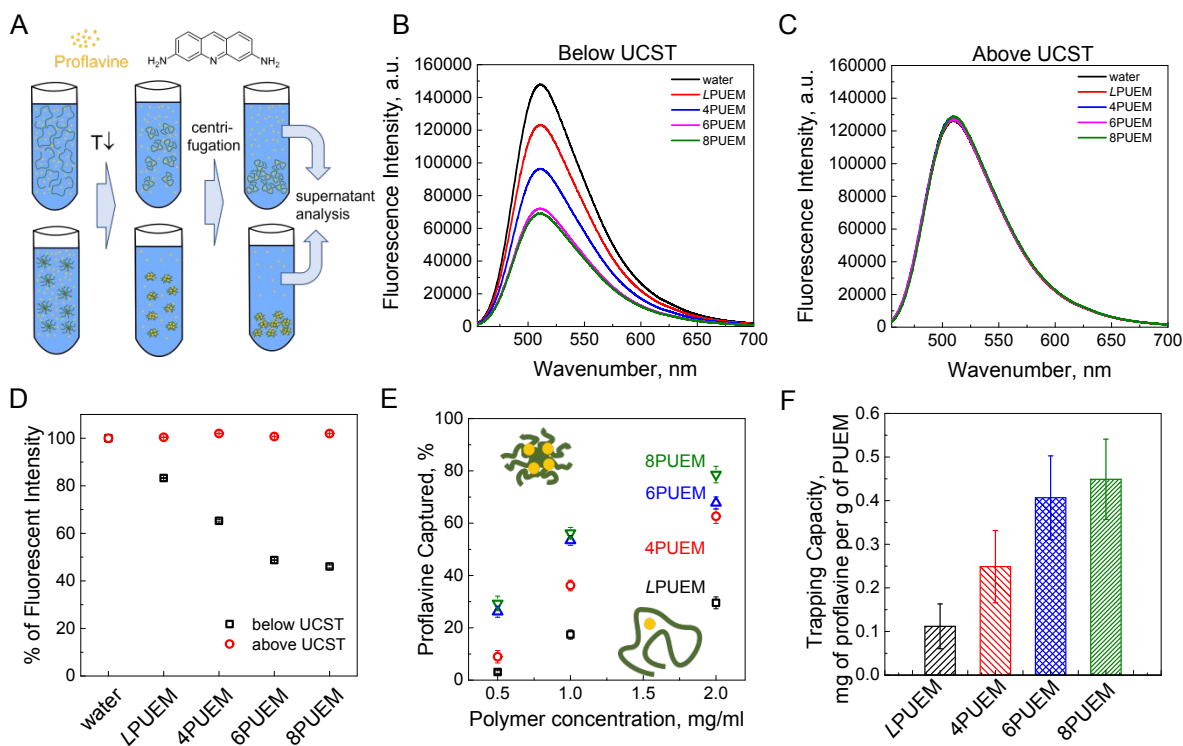
Fig. 7. (A) Schematic representation of trapping of proflavine within PUEMs. Fluorescence emission spectra (λ_{ex}=445 nm) of proflavine supernatant solutions after centrifugation of 1 mg/ml solution of linear, 4, 6 and 8-arm PUEM at 5 °C (B) and 75 °C (C) at pH 6. (D) Percentage of fluorescence intensity of proflavine remaining in water or 1 mg/ml PUEM polymer solutions after centrifugation below UCST (5 °C, squares) or above UCST (75°C, circles). (E) Percentage of captured proflavine as a function of polymer concentration for linear (squares), 4-arm (circles), 6-arm (up-pointing triangles) and 8-arm (down-pointing triangles) PUEMs at 5°C. (F) Trapping capacity of proflavine hydrochloride per gram of linear and star PUEMs. All solutions were adjusted to pH 6.

temperature; the solutions were then cooled to 5 °C and centrifuged to separate the precipitated polymers with trapped proflavine. **Fig. 7B** shows that fluorescence intensity of proflavine remaining in the supernatant decreased with number of arms in PUEMs, suggesting that higher amounts of the dye were trapped by more branched polymers. At the same time, all proflavine remained in solution at 75 °C (**Fig. 7C).** This result, obtained with 1 mg/ml PUEM solutions, is further illustrated by **Fig. 7D**. Similar trends were also observed with higher and lower PUEM concentrations (**Fig. S16**). **Fig. 7E** and **Fig. S17** illustrate that the percentage of proflavine trapped within the phase separated PUEMs was higher for more branched PUEMs and increased with

PUEM concentration. **Fig. 7F** summarizes the trapping capacity of proflavine (calculated as mg of proflavine per g of PUEM) for polymers with different molecular architectures, showing that 8-arm PUEM was able to trap ~4.5-fold more proflavine than its linear counterpart, *L*PUEM. This result further confirms the importance of the higher local concentration provided by the star architecture for proflavine trapping. Importantly, interactions of the dye with the phase-separated PUEMs could be revealed via a ~4 nm blue shift of the emission peak of proflavine as compared to its fluorescence in water (**Fig. S18**). A similar blue shift in proflavine fluorescence was observed upon its binding with cucurbiturils via hydrophobic and hydrogen bonding interactions.[64-65] It is likely that similar interactions occur between proflavine and PUEMs, which dehydrate, form polymer-polymer hydrogen bonds and provide hydrophobic environment for inclusion of the dye.[36] At the same time, the higher density of polymer units in star polymers supports stronger binding and higher trapping capacity of proflavine.

The existence of hydrophobic domains in collapsed PUEMs was more directly confirmed in the experiments with pyrene – a dye whose fluorescence is highly sensitive to hydrophobicity/hydrophilicity of the environment.[36] In particular, fluorescence of pyrene experiences a bathochromic shift in less polar environments, and this shift can be observed in the excitation spectra.[66] **Fig. 8** shows the excitation spectra of pyrene in solutions of linear and star PUEMs. In these experiments, solutions of CTAB micelles, whose excitation spectra demonstrate a characteristic red shift after inclusion of pyrene within hydrophobic micellar cores, were used as control.[36, 67] Below UCST transition, the fluorescence peaks in the excitation spectra of pyrene in contact with all PUEMs shifted to longer wavelengths in comparison to water, suggesting that the polymers contained domains for entrapped pyrene molecules via hydrophobic interactions. Similarly to experiments with proflavine, trapping of pyrene was fully reversible and the red shift in the fluorescent spectra of pyrene emission inverted to those observed in polymer-free pyrene solutions when temperature was raised above the UCST transition of PEUM polymers (**Figs. 8A and S19**). Importantly, below UCST the magnitude of the red shift in fluorescence was larger for the star polymers and increased with number of arms, confirming more efficient inclusion of pyrene within the hydrophobic domains of collapsed PUEMs. The data suggests that the more compact structure of star polymers was favorable for the formation of such hydrophobic domains and dye inclusion.
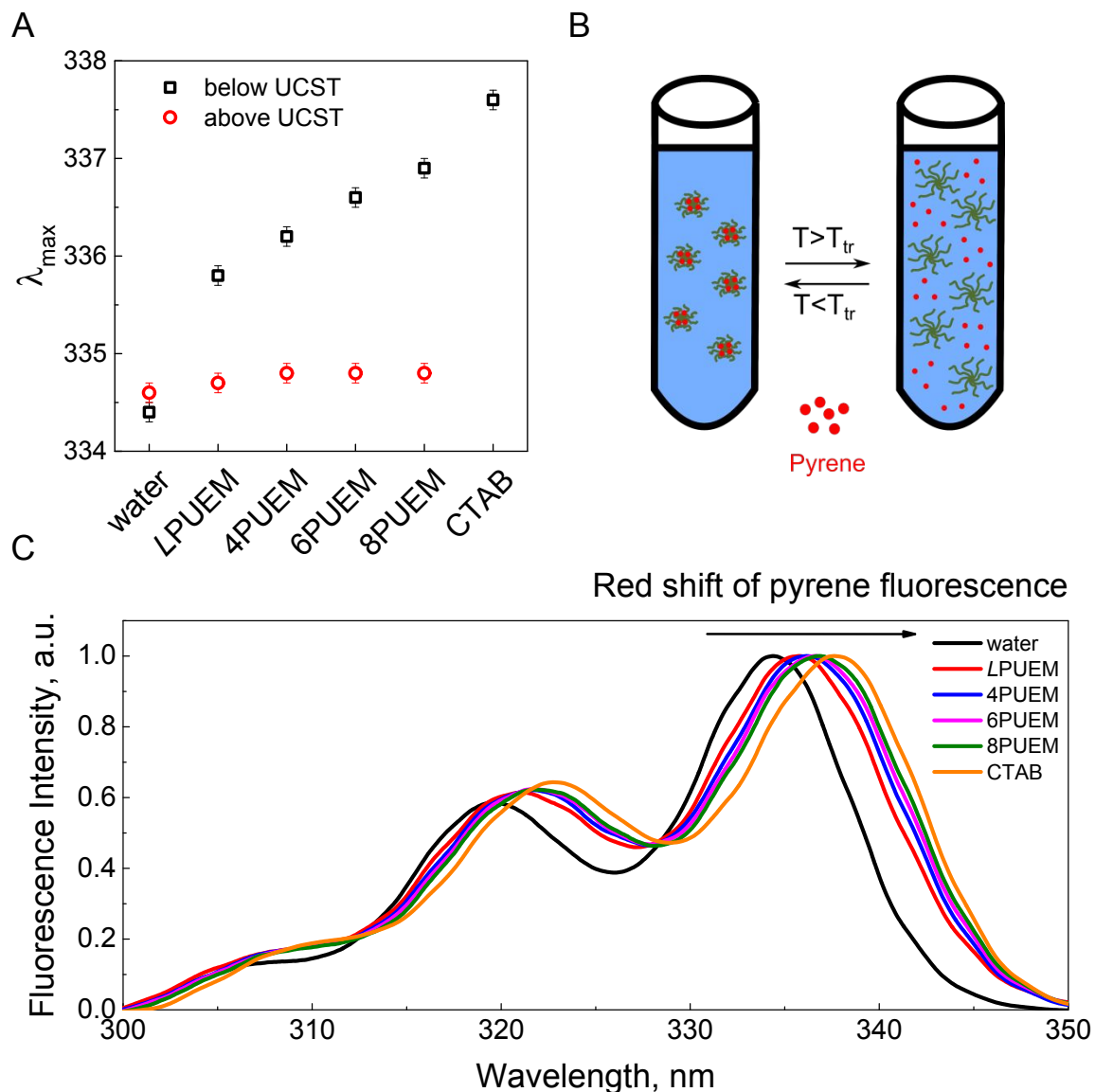
Fig. 8. (A) Excitation wavelength of pyrene fluorescence below and above UCST transition temperature in 1 mg/ml solutions of linear and star PUEMs. (B) Schematic representation of capture and release of pyrene by a UCST star polymer. (C) Fluorescence excitation spectra of pyrene (λ_{em} = 392 nm) detected in water and 1 mg/ml aqueous solutions of CTAB, linear or star PUEMs at 5 °C. All solutions were adjusted to pH 6.

Conclusion

In summary, we implemented the ARGET ATRP technique to synthesize star-shaped UCST polymers of the matched molecular weight using core-first approach and demonstrated that

the procedure yields polymers with well controlled branching. Our experiments revealed that polymer architecture of PUEMs with relatively low branching (up to 8 arms) did not significantly affect the polymer UCST behavior. At the same time, the addition of DMSO – a competitive hydrogen bonding molecule — significantly affected the transition temperature in both linear and star PUEMs, enabling to precisely control UCST behavior in PUEM aqueous solutions via DMSO concentration. While the transition temperatures of PUEMs with all molecular architectures were similar in mixed DMSO/water solvents, a dramatic effect of molecular architecture was observed in trapping of fluorescent model molecules – proflavine and pyrene – by the phase-separating PUEM molecules. Our experiments revealed more efficient trapping of the dyes by star PUEMs due to their high local density of the polymer units. Moreover, experiments with inclusion of pyrene indicated that PUEMs with larger number of arms created more hydrophobic environments within UCST-collapsed molecules and that these environments favored inclusion of hydrophobic dyes. The fully reversible nature of such trapping can be exploited for designing novel temperature-responsive drug delivery systems.

References:

1.   Seuring, J.; Agarwal, S., Polymers with Upper Critical Solution Temperature in Aqueous Solution. *Macromolecular Rapid Communications* **2012,** *33* (22), 1898-1920.

2.   Niskanen, J.; Tenhu, H., How to manipulate the upper critical solution temperature (UCST)? *Polymer Chemistry* **2017,** *8* (1), 220-232.

3.   Seuring, J.; Agarwal, S., Polymers with Upper Critical Solution Temperature in Aqueous Solution: Unexpected Properties from Known Building Blocks. *ACS Macro Letters* **2013,** *2* (7), 597-600.

4.   Zhao, C.; Ma, Z.; Zhu, X. X., Rational design of thermoresponsive polymers in aqueous solutions: A thermodynamics map. *Progress in Polymer Science* **2019,** *90*, 269-291.

5.   Seuring, J.; Agarwal, S., Non-Ionic Homo- and Copolymers with H-Donor and H-Acceptor Units with an UCST in Water. *Macromolecular Chemistry and Physics* **2010,** *211* (19), 2109-2117.

6.   Asadujjaman, A.; Kent, B.; Bertin, A., Phase transition and aggregation behaviour of an UCST-type copolymer poly(acrylamide-co-acrylonitrile) in water: effect of acrylonitrile content, concentration in solution, copolymer chain length and presence of electrolyte. *Soft Matter* **2017,** *13* (3), 658-669.

7.   Glatzel, S.; Laschewsky, A.; Lutz, J.-F., Well-Defined Uncharged Polymers with a Sharp UCST in Water and in Physiological Milieu. *Macromolecules* **2011,** *44* (2), 413-415.

8.   Zhang, G.; Wang, Y.; Liu, G., Poly(3-imidazolyl-2-hydroxypropyl methacrylate) – a new polymer with a tunable upper critical solution temperature in water. *Polymer Chemistry* **2016,** *7* (43), 6645-6654.

9.   Shimada, N.; Ino, H.; Maie, K.; Nakayama, M.; Kano, A.; Maruyama, A., Ureido-Derivatized Polymers Based on Both Poly(allylurea) and Poly(l-citrulline) Exhibit UCST-Type Phase Transition Behavior under Physiologically Relevant Conditions. *Biomacromolecules* **2011,** *12* (10), 3418-3422.

10.   Meiswinkel, G.; Ritter, H., A New Type of Thermoresponsive Copolymer with UCST-Type Transitions in Water: Poly(N-vinylimidazole-co-1-vinyl-2-(hydroxymethyl)imidazole). *Macromolecular Rapid Communications* **2013,** *34* (12), 1026-1031.

11.   Mishra, V.; Jung, S.-H.; Jeong, H. M.; Lee, H.-i., Thermoresponsive ureido-derivatized polymers: the effect of quaternization on UCST properties. *Polymer Chemistry* **2014,** *5* (7), 2411-2416.

12.   Zhao, C.; Dolmans, L.; Zhu, X. X., Thermoresponsive Behavior of Poly(acrylic acid-co-acrylonitrile) with a UCST. *Macromolecules* **2019,** *52* (12), 4441-4446.

13.   Liu, F.; Seuring, J.; Agarwal, S., Controlled radical polymerization of N-acryloylglycinamide and UCST-type phase transition of the polymers. *Journal of Polymer Science Part A: Polymer Chemistry* **2012,** *50* (23), 4920-4928.

14.   Zhang, M.; Shen, W.; Xiong, Q.; Wang, H.; Zhou, Z.; Chen, W.; Zhang, Q., Thermo-responsiveness and biocompatibility of star-shaped poly[2-(dimethylamino)ethyl methacrylate]-b-poly(sulfobetaine methacrylate) grafted on a β-cyclodextrin core. *RSC Advances* **2015,** *5* (36), 28133-28140.

15.   Huang, G.; Li, H.; Feng, S.-T.; Li, X.; Tong, G.; Liu, J.; Quan, C.; Jiang, Q.; Zhang, C.; Li, Z., Self-assembled UCST-Type Micelles as Potential Drug Carriers for Cancer Therapeutics. *Macromolecular Chemistry and Physics* **2015,** *216* (9), 1014-1023.

16.   Palanisamy, A.; Sukhishvili, S. A., Swelling Transitions in Layer-by-Layer Assemblies of UCST Block Copolymer Micelles. *Macromolecules* **2018,** *51* (9), 3467-3476.

17.   Palanisamy, A.; Albright, V.; Sukhishvili, S. A., Upper Critical Solution Temperature Layer-by-Layer Films of Polyamino acid-Based Micelles with Rapid, On-Demand Release Capability. *Chemistry of Materials* **2017,** *29* (21), 9084-9094.

18.   Aliakseyeu, A.; Albright, V.; Yarbrough, D.; Hernandez, S.; Zhou, Q.; Ankner, J. F.; Sukhishvili, S. A., Selective hydrogen bonding controls temperature response of layer-by-layer upper critical solution temperature micellar assemblies. *Soft Matter* **2021,** *17* (8), 2181-2190.

19.   Albright, V.; Palanisamy, A.; Zhou, Q.; Selin, V.; Sukhishvili, S. A., Functional Surfaces through Controlled Assemblies of Upper Critical Solution Temperature Block and Star Copolymers. *Langmuir* **2019,** *35* (33), 10677-10688.

20.   Ren, J. M.; McKenzie, T. G.; Fu, Q.; Wong, E. H. H.; Xu, J.; An, Z.; Shanmugam, S.; Davis, T. P.; Boyer, C.; Qiao, G. G., Star Polymers. *Chemical Reviews* **2016,** *116* (12), 6743-6836.

21.   Chremos, A.; Douglas, J. F., Solution properties of star polyelectrolytes having a moderate number of arms. *The Journal of Chemical Physics* **2017,** *147* (4), 044906.

22.   Poree, D. E.; Giles, M. D.; Lawson, L. B.; He, J.; Grayson, S. M., Synthesis of Amphiphilic Star Block Copolymers and Their Evaluation as Transdermal Carriers. *Biomacromolecules* **2011,** *12* (4), 898-906.

23.   Tungala, K.; Adhikary, P.; Azmeera, V.; Kumar, K.; Krishnamoorthi, S., Dendritic star polymer of polyacrylamide based on a β-cyclodextrin trimer: a flocculant and drug vehicle. *New Journal of Chemistry* **2017,** *41* (2), 611-618.

24.   Zhang, Y.; Yan, J.; Avellan, A.; Gao, X.; Matyjaszewski, K.; Tilton, R. D.; Lowry, G. V., Temperature- and pH-Responsive Star Polymers as Nanocarriers with Potential for in Vivo Agrochemical Delivery. *ACS Nano* **2020,** *14* (9), 10954-10965.

25.   Shi, X.; Ma, X.; Hou, M.; Gao, Y.-E.; Bai, S.; Xiao, B.; Xue, P.; Kang, Y.; Xu, Z.; Li, C. M., pH-Responsive unimolecular micelles based on amphiphilic star-like copolymers with high drug loading for effective drug delivery and cellular imaging. *Journal of Materials Chemistry B* **2017,** *5* (33), 6847-6859.

26.   Yokoyama, H.; Takano, A.; Okada, M.; Nose, T., Phase diagram of star-shaped polystyrene/cyclohexane system: location of critical point and profile of coexistence curve. *Polymer* **1991,** *32* (17), 3218-3224.

27.   Alessi, M. L.; Bittner, K. C.; Greer, S. C., Eight-arm star polystyrene in methylcyclohexane: Cloud-point curves, critical lines, and coexisting densities and viscosities. *Journal of Polymer Science Part B: Polymer Physics* **2004,** *42* (1), 129-145.

28.   Jacobs, D. T.; Braganza, C. I.; Brinck, A. P.; Cohen, A. B.; Lightfoot, M. A.; Locke, C. J.; Suddendorf, S. J.; Timmers, H. R.; Triplett, A. L.; Venkataraman, N. L.; Wellons, M. T., Universality in eight-arm star polystyrene and methylcyclohexane mixtures near the critical point. *The Journal of Chemical Physics* **2007,** *127* (12), 124905.

29.   Numasawa, N.; Okada, M., Coexistence Curve of a Star-Shaped Polymer Solution. Comparison with the Hybrid Theory. *Polymer Journal* **1999,** *31* (1), 99-101.

30.   Cowie, J. M. G.; Horta, A.; McEwen, I. J.; Prochazka, K., Upper and lower critical solution temperatures for star branched polystyrene in cyclohexane. *Polymer Bulletin* **1979,** *1* (5), 329-335.

31.   Arya, G.; Panagiotopoulos, A. Z., Impact of Branching on the Phase Behavior of Polymers. *Macromolecules* **2005,** *38* (25), 10596-10604.

32.   Horta, A.; Pastoriza, M. A., The interaction parameter of crosslinked networks and star polymers. *European Polymer Journal* **2005,** *41* (12), 2793-2802.

33.   Zhou, Q.; Palanisamy, A.; Albright, V.; Sukhishvili, S. A., Enzymatically degradable star polypeptides with tunable UCST transitions in solution and within layer-by-layer films. *Polymer Chemistry* **2018,** *9* (40), 4979-4983.

34.   Li, Z.; Li, H.; Sun, Z.; Hao, B.; Lee, T.-C.; Feng, A.; Zhang, L.; Thang, S. H., Synthesis of star-shaped polyzwitterions with adjustable UCST and fast responsiveness by a facile RAFT polymerization. *Polymer Chemistry* **2020,** *11* (18), 3162-3168.

35.   Qi, M.; Li, K.; Zheng, Y.; Rasheed, T.; Zhou, Y., Hyperbranched Multiarm Copolymers with a UCST Phase Transition: Topological Effect and the Mechanism. *Langmuir* **2018,** *34* (9), 3058-3067.

36.   Fujihara, A.; Itsuki, K.; Shimada, N.; Maruyama, A.; Sagawa, N.; Shikata, T.; Yusa, S.-I., Preparation of ureido group bearing polymers and their upper critical solution temperature in water. *Journal of Polymer Science Part A: Polymer Chemistry* **2016,** *54* (18), 2845-2854.

37.   Fujihara, A.; Shimada, N.; Maruyama, A.; Ishihara, K.; Nakai, K.; Yusa, S.-i., Preparation of upper critical solution temperature (UCST) responsive diblock copolymers bearing pendant ureido groups and their micelle formation behavior in water. *Soft Matter* **2015,** *11* (26), 5204-5213.

38.   Ohshio, M.; Ishihara, K.; Maruyama, A.; Shimada, N.; Yusa, S.-i., Synthesis and Properties of Upper Critical Solution Temperature Responsive Nanogels. *Langmuir* **2019,** *35* (22), 7261-7267.

39.   Kitano, K.; Ishihara, K.; Yusa, S.-i., Preparation of a thermo-responsive drug carrier consisting of a biocompatible triblock copolymer and fullerene. *Journal of Materials Chemistry B* **2022**.

40.   Shendage, D. M.; Fröhlich, R.; Haufe, G., Highly Efficient Stereoconservative Amidation and Deamidation of α-Amino Acids. *Organic Letters* **2004,** *6* (21), 3675-3678.

41.   Ramirez, R.; Woodcock, J.; Kilbey, S. M., ARGET-ATRP synthesis and swelling response of compositionally varied poly(methacrylic acid-co-N,N-diethylaminoethyl methacrylate) polyampholyte brushes. *Soft Matter* **2018,** *14* (30), 6290-6302.

42.   Zimm, B. H.; Kilb, R. W., Dynamics of branched polymer molecules in dilute solution. *Journal of Polymer Science* **1959,** *37* (131), 19-42.

43.   Barner-Kowollik, C.; Davis, T. P.; Stenzel, M. H., Synthesis of Star Polymers using RAFT Polymerization: What is Possible? *Australian Journal of Chemistry* **2006,** *59* (10), 719-727.

44.   Matyjaszewski, K.; Woodworth, B. E., Interaction of Propagating Radicals with Copper(I) and Copper(II) Species. *Macromolecules* **1998,** *31* (15), 4718-4723.

45.   Jakubowski, W.; Matyjaszewski, K., Activators Regenerated by Electron Transfer for Atom-Transfer Radical Polymerization of (Meth)acrylates and Related Block Copolymers. *Angewandte Chemie International Edition* **2006,** *45* (27), 4482-4486.

46.   Matyjaszewski, K.; Jakubowski, W.; Min, K.; Tang, W.; Huang, J.; Braunecker, W. A.; Tsarevsky, N. V., Diminishing catalyst concentration in atom transfer radical polymerization with reducing agents. *Proceedings of the National Academy of Sciences* **2006,** *103* (42), 15309-15314.

47.   Taton, D.; Gnanou, Y.; Matmour, R.; Angot, S.; Hou, S.; Francis, R.; Lepoittevin, B.; Moinard, D.; Babin, J., Controlled polymerizations as tools for the design of star-like and dendrimer-like polymers. *Polymer International* **2006,** *55* (10), 1138-1145.

48.   Alidedeoglu, A. H.; York, A. W.; McCormick, C. L.; Morgan, S. E., Aqueous RAFT polymerization of 2-aminoethyl methacrylate to produce well-defined, primary amine functional homo- and copolymers. *Journal of Polymer Science Part A: Polymer Chemistry* **2009,** *47* (20), 5405-5415.

49.   Thompson, K. L.; Read, E. S.; Armes, S. P., Chemical degradation of poly(2-aminoethyl methacrylate). *Polymer Degradation and Stability* **2008,** *93* (8), 1460-1466.

50.   He, L.; Read, E. S.; Armes, S. P.; Adams, D. J., Direct Synthesis of Controlled-Structure Primary Amine-Based Methacrylic Polymers by Living Radical Polymerization. *Macromolecules* **2007,** *40* (13), 4429-4438.

51.   Mendonça, P. V.; Averick, S. E.; Konkolewicz, D.; Serra, A. C.; Popov, A. V.; Guliashvili, T.; Matyjaszewski, K.; Coelho, J. F. J., Straightforward ARGET ATRP for the Synthesis of Primary Amine Polymethacrylate with Improved Chain-End Functionality under Mild Reaction Conditions. *Macromolecules* **2014,** *47* (14), 4615-4621.

52.   Parker, F. S., Amides and Amines. In *Applications of Infrared Spectroscopy in Biochemistry, Biology, and Medicine*, Parker, F. S., Ed. Springer US: Boston, MA, 1971; pp 165-172.

53.   Seuring, J.; Bayer, F. M.; Huber, K.; Agarwal, S., Upper Critical Solution Temperature of Poly(N-acryloyl glycinamide) in Water: A Concealed Property. *Macromolecules* **2012,** *45* (1), 374-384.

54.　　　Wang, Y.; He, J.; Aktas, S.; Sukhishvili, S. A.; Kalyon, D. M., Rheological behavior and self-healing of hydrogen-bonded complexes of a triblock Pluronic® copolymer with a weak polyacid. *Journal of Rheology* **2017,** *61* (6), 1103-1119.

55.　　　Selin, V.; Aliakseyeu, A.; Ankner, J. F.; Sukhishvili, S. A., Effect of a Competitive Solvent on Binding Enthalpy and Chain Intermixing in Hydrogen-Bonded Layer-by-Layer Films. *Macromolecules* **2019,** *52* (12), 4432-4440.

56.　　　Gao, H., Development of Star Polymers as Unimolecular Containers for Nanomaterials. *Macromolecular Rapid Communications* **2012,** *33* (9), 722-734.

57.　　　Yang, D.-P.; Oo, M. N. N. L.; Deen, G. R.; Li, Z.; Loh, X. J., Nano-Star-Shaped Polymers for Drug Delivery Applications. *Macromolecular Rapid Communications* **2017,** *38* (21), 1700410.

58.　　　Flemming, P.; Münch, A. S.; Fery, A.; Uhlmann, P., Constrained thermoresponsive polymers – new insights into fundamentals and applications. *Beilstein Journal of Organic Chemistry* **2021,** *17*, 2123-2163.

59.　　　Le, M.; Huang, W.; Chen, K.-F.; Lin, C.; Cai, L.; Zhang, H.; Jia, Y.-G., Upper critical solution temperature polymeric drug carriers. *Chemical Engineering Journal* **2022,** *432*, 134354.

60.　　　Sponchioni, M.; Capasso Palmiero, U.; Moscatelli, D., Thermo-responsive polymers: Applications of smart materials in drug delivery and tissue engineering. *Materials Science and Engineering: C* **2019,** *102*, 589-605.

61.　　　Kožurková, M.; Sabolová, D.; Kristian, P., A review on acridinylthioureas and its derivatives: biological and cytotoxic activity. *Journal of Applied Toxicology* **2017,** *37* (10), 1132-1139.

62.　　　Sabolova, D.; Kristian, P.; Kozurkova, M., Proflavine/acriflavine derivatives with versatile biological activities. *Journal of Applied Toxicology* **2020,** *40* (1), 64-71.

63.　　　Dsouza, R. N.; Pischel, U.; Nau, W. M., Fluorescent Dyes and Their Supramolecular Host/Guest Complexes with Macrocycles in Aqueous Solution. *Chemical Reviews* **2011,** *111* (12), 7941-7980.

64.　　　Kemp, S.; Wheate, N. J.; Stootman, F. H.; Aldrich-Wright, J. R., The Host-Guest Chemistry of Proflavine with Cucurbit[6,7,8]urils. *Supramolecular Chemistry* **2007,** *19* (7), 475-484.

65.   Chakraborty, B.; Basu, S., Deciphering the host–guest chemistry of Acridine Yellow and Cucurbit[7]uril: An integrated spectroscopic and calorimetric study. *Chemical Physics Letters* **2011,** *507* (1), 74-79.

66.   Wilhelm, M.; Zhao, C. L.; Wang, Y.; Xu, R.; Winnik, M. A.; Mura, J. L.; Riess, G.; Croucher, M. D., Poly(styrene-ethylene oxide) block copolymer micelle formation in water: a fluorescence probe study. *Macromolecules* **1991,** *24* (5), 1033-1040.

67.   Xu, L.; Zhu, Z.; Sukhishvili, S. A., Polyelectrolyte Multilayers of Diblock Copolymer Micelles with Temperature-Responsive Cores. *Langmuir* **2011,** *27* (1), 409-415.